Homeobox Protein *Hop* Functions in the Adult Cardiac Conduction System

Fraz A. Ismat, **Maozhen Zhang**, **Hyun Kook**, **Bin Huang**, **Rong Zhou**, **Victor A. Ferrari**, **Jonathan A. Epstein**, and **Vickas V. Patel**

From the Division of CardiologyDepartment of Pediatrics, The Children's Hospital of Philadelphia, Philadelphia, Pa

Division of Cardiovascular Medicine

Department of RadiologyUniversity of Pennsylvania, Philadelphia, Pa

the Department of Pharmacology and Medical Research Center for Gene Regulation Chonnam National University Medical School, Gwangju, South Korea.

Abstract

Hop is an unusual homeobox gene expressed in the embryonic and adult heart. *Hop* acts downstream of *Nkx2–5* during development, and *Nkx2–5* mutations are associated with cardiac conduction system (CCS) defects. Inactivation of *Hop* in the mouse is lethal in half of the expected null embryos. Here, we show that *Hop* is expressed strongly in the adult CCS. $Hop^{-/-}$ adult mice display conduction defects below the atrioventricular node (AVN) as determined by invasive electrophysiological testing. These defects are associated with decreased expression of connexin40. Our results suggest that *Hop* functions in the adult CCS and demonstrate conservation of molecular hierarchies between embryonic myocardium and the specialized conduction tissue of the mature heart.

Keywords

Hop; conduction; connexin40; Nkx2—5; mouse mutants

Synchronized contraction of the atrial and ventricular chambers is essential for normal cardiac function, and the cardiac conduction system (CCS) is required for mediating this delicate interplay. However, little is known about the molecular cascades regulating CCS development and function. Several studies suggest that certain components of the avian CCS are locally derived from bipotential cardiomyogenic cells.[1] Endothelin, neuregulin-1, and *Nkx2–5* have each been implicated as contributors to the transition between ventricular and conductive cell lineages in animals.[2–5] Additionally, patients with mutations in *Nkx2–5* exhibit congenital heart defects and conduction system disease, notable for progressive atrioventricular block.[6] Complete loss of *Nkx2–5* leads to loss of the atrioventricular node (AVN) anlage,[5] and a mouse model in which *Nxk2–5* has been selectively removed from the ventricular myocardium demonstrates hypoplasia and progressive loss of cells from the AVN along with atrioventricular block.[4]

We and others recently identified *Hop*, a novel homeodomain protein in the embryonic heart functioning downstream of *Nkx2–5*.[7,8] *Hop* encodes a 73 amino acid protein that contains a domain (the 60 amino acid homeodomain) homologous to those seen in homeobox (*Hox*)

Correspondence to Vickas V. Patel, MD, PhD, 906 Biomedical Research Bldg II/III, 421 Curie Blvd, Philadelphia, PA 19104. E-mail vickas.patel@uphs.upenn.edu.

transcription factors. Unlike all other known *Hox* transcription factors, *Hop* does not directly bind DNA.[9] *Hop* is known to interact with serum response factor (SRF) and interfere with SRF-mediated gene transcription.[7,8] Mice lacking *Hop* (*Hop*$^{-/-}$) are born at ≈50% of the expected frequency, with loss of embryos between E10.5 and E12.5.[7] *Hop* expression also continues into the postnatal period and transgenic overexpression in adult myocardium leads to cardiac hypertrophy and heart failure.[9] In this study, we present evidence that *Hop* is highly expressed in the adult mouse CCS and is required for proper function during adulthood.

Materials and Methods

Animals

Creation of *Hop* knockout mice (*Hop*$^{-/-}$) has been recently described.[7] Mice were bred on a mixed C57BL/6 and 129sv background (Jackson Laboratories, Bar Harbor, Me). All protocols conformed to the guidelines established by the Association for the Assessment and Accreditation of Laboratory Animal Care and were approved by the University of Pennsylvania Animal Care and Use Committees.

β-Galactosidase Activity Staining

Specimens were stained for β-galactosidase activity using a previously described protocol,[13] both for whole-mounted tissue and individual slides, as noted.

Acetylcholinesterase Activity Staining

Staining for acetylcholinesterase activity was performed using a previously described protocol.[14]

Connexing40 Protein Quantification

The superior portion of the interventricular septum was isolated from adult littermates (*Hop*$^{+/+}$, *Hop*$^{+/-}$, and *Hop*$^{-/-}$). Western blots using anti-connexin40 antibody at 1 mcg/mL (Chemicon) and anti–α-tubulin antibody at 0.1 μg/mL (Sigma) were quantified using ImageJ software (NIH).

Immunohistochemistry

Frozen sections of hearts from *Hop*$^{+/-}$ and *Hop*$^{-/-}$ mice were stained for connexin40. Hearts were embedded unfixed. Slides were air dried, fixed with 4% paraformaldehyde, washed with PBS, and briefly dehydrated through an ethanol series and then rehydrated before washes with PBST (PBS +0.5% Tween-20). They were then blocked with 10% goat serum in PBST, incubated with anti-Cx40 antibody 1:100 in 5% goat serum in 0.1%PBST, washed in PBS, and incubated with fluorescent secondary antibody at 1:500 (Molecular Probes).

Cardiac-Gated Magnetic Resonance Imaging

Hop$^{-/-}$ and wild-type mice underwent cardiac-gated magnetic resonance imaging (MRI) to compare left ventricular morphology and function, as previously described.[18] Left ventricular (LV) wall thickness, mass, and ejection fraction were measured in the short-axis planes.

EPS Preparation and Protocol

Surface ECG and invasive mouse electrophysiology studies were performed as previously described.[15,16] Briefly, surface ECG recordings and complete in vivo electrophysiological studies (EPS) were obtained from *Hop*$^{-/-}$ adult mice (10 to 14 weeks old) and age-matched *Hop*$^{+/+}$ littermates. Each mouse was anesthetized with pentobarbital (0.033 mg/kg IP), and multi-lead ECGs were obtained using 26-gauge subcutaneous electrodes. A jugular vein

cutdown was performed and an octapolar 2-French electrode catheter (CIBer mouse-EP; NuMED, Inc) placed in the right atrium and ventricle under electrogram guidance to confirm catheter position. A programmed digital stimulator (DTU-215A, Bloom Associates Ltd) was used to deliver electrical impulses at approximately twice diastolic threshold. Surface ECG and intra-cardiac electrograms were simultaneously displayed on a multi-channel oscilloscope recorder (Quinton Electrophysiology, Inc) at a digitization rate of 2 kHz and stored on optical media for offline analysis. ECG channels were filtered from 0.5 to 250 Hz and intracardiac electrograms were filtered from 5 to 400 Hz. ECG intervals were measured by two independent observers blinded to the animal's genotype.

Ambulatory ECG Recordings

Ambulatory ECG recordings were obtained by aseptic, subcutaneous implantation of a 3.5-g wireless radiofrequency telemetry device (Data Sciences International) configured to record a signal analogous to ECG lead I as previously described.[17] Following a 72-hour recovery period after surgical instrumentation, ECG recordings were obtained from $Hop^{-/-}$ and $Hop^{+/+}$ mice, each placed in a separate cage overlying a receiver.

CCS Volume Calculations

Digital photomicrographs of all sections through the AVN and proximal CCS were obtained with an Axiophot2 microscope (Carl Zeiss) and Nikon DXM1200 digital camera after staining for β-galactosidase activity. The structural regions of the CCS were defined according to the method of Rentschler et al[10] where stained sections above the bifurcation of the bundle branches, encompassed by atrial tissues, were taken as the AVN and stained tissues distal to the AVN, but proximal to the division of the bundle branches, were taken as the His-bundle. Measurement of the area of interest (the AVN proper and His-bundle) was performed with ImageJ software. The sum of the areas of interest multiplied by the section thickness (6 to 8 μm) was used to compute the estimated volume.

Quantitative RT-PCR

Quantitative RT-PCR was performed using SYBR Green according to the manufacturer's protocol. Total RNA was isolated from whole hearts for real-time RT-PCR with TRIzol (Invitrogen, Inc). PCR was preformed with 5 μL of reverse transcribed cDNA reaction mixture, 400 nmol/L of specific forward and reverse primers and 1xSYBR Green PCR Master Mix (Applied Biosystems, Inc.). The following primer pairs were used: (1) connexin40 (Cx40), 5′-ACAAGCACTCCACAGTCATCGGC-3′ and 5′-AGCAGGACAGCTCGGCCTTTTC-3′; (2) connexin43 (Cx43), 5′-CCTTGGGGAAGCTGCTGGACAA-3′ and 5′-CAGCAGGCCACCTCTCATCTTCA-3′; (3) glyceraldehyde-3-phosphate dehydrogenase (GAPDH), 5′-GTGGCAAAGTGGATTGTTGCC-3′ and 5′-GATGATGACCCGTTTGGCTCC-3′. Quantification of the reaction product was performed using the MJ Research DNA Engine Opticon 2 real-time detection system. PCR cycle conditions were 95°C for 10 minutes, followed by 40 cycles of denaturation at 95°C for 15 seconds and annealing and extension at 60°C for 1 minute. All reactions were performed in triplicate with and without RT as controls. Cycle threshold values were converted to relative gene expression levels using the $2^{-\Delta\Delta C(t)}$ method.

Statistical Analysis

Continuous variables, such as ECG intervals and cardiac conduction properties, were compared using a two-tailed Student *t* test. All values are reported as the mean±1SD, unless otherwise noted. A probability value <0.05 was considered significant.

Results

Hop Expression in the Adult Murine Heart

During embryonic development, *Hop* is strongly expressed throughout the developing heart. [7,8] Insertion of the *lacZ* gene into the endogenous *Hop* locus allowed us to detect sites of expression with high sensitivity. Gross examination of hearts from adult *Hop*^{−/−} and *Hop*^{+/−} mice stained for β-galactosidase activity demonstrated strong expression within the cardiac conduction system (Figure 1A through 1F). This pattern of expression appears to overlap with that of CCS-LacZ[10] and MinK-LacZ mice,[11] which each demarcate regions of the CCS. This CCS-delimited staining pattern was less prominent in newborn mice (Figure 1G and 1H) where there was more prominent staining throughout the myocardium as compared with adults, but more restricted to the endocardium and interventricular septum than during embryogenesis. Additionally, uniform expression of β-galactosidase activity was detected in the atria of *Hop*^{+/−} and *Hop*^{−/−} hearts (Figure 1I and 1J). Staining of adjacent sections with β-galactosidase and for AchE activity confirmed expression of *Hop* within the proximal CCS (Figure 1K through 1M). The hearts of adult *Hop*^{−/−} mice were structurally normal and had normal function as assessed by invasive hemodynamic monitoring[9] and cardiac-gated MRI (Table 1). Quantitative morphometric analysis of proximal CCS volume in *Hop*^{−/−} and *Hop*^{+/−} hearts suggested that proximal CCS tissue integrity was maintained in null animals (Table 2).

ECG and Electrophysiologic Analysis of *Hop*^{−/−} Mice

With our initial anatomical observations, we sought to determine whether *Hop* played a functional role in cardiac conduction. ECG analysis revealed a wider QRS-complex, longer QT-interval, and wider p-wave in *Hop*^{−/−} mice compared with wild-type mice (Figure 2A through 2D). Resting heart rates and baseline PR-intervals were similar between *Hop*^{−/−} and wild-type mice. In addition, ECG recordings in 5 of 10 *Hop*^{−/−} mice showed right axis deviation that was not present in any wild-type littermates. Similar findings were seen in unsedated, ambulatory ECG recordings (Table 3) with no evidence of spontaneous arrhythmias in either group.

Intracardiac EPS revealed a longer HV interval in *Hop*^{−/−} mice compared with wild-type controls, whereas the AH interval trended toward being longer in *Hop*^{−/−} mice but did not reach statistical significance. These results suggest that conduction delay accounting for the widened QRS complex on surface ECGs is due predominantly to defective conduction below the AVN and is consistent with strong expression of *Hop* in the infra-His region and bundle branches. In addition, the atrial effective refractory period (AERP) was prolonged in *Hop*^{−/−} mice (Table 4).

Connexin40 Expression Is Reduced in Adult *Hop*^{−/−} Mice

Because cardiac connexin expression is dependent on proper expression of *Nkx2–5* in the heart and *Hop* functions downstream of *Nkx2–5*, we sought to determine whether deletion of *Hop* might also affect expression of cardiac connexins. RT-PCR analysis showed a significant reduction in Cx40/GAPDH normalized mRNA expression in hearts from *Hop*^{−/−} mice versus wild-type littermates (1.64 ± 0.06 versus 2.31 ± 0.13; $P<0.01$). However, Cx43/GAPDH normalized mRNA was not different in the hearts of *Hop*^{−/−} mice compared with littermate controls and similar results were obtained from microarray analysis (data not shown). Further, there was a reduction of connexin40 protein in the proximal CCS of *Hop*^{−/−} mice, whereas there was no difference between wild-type and *Hop*^{+/−} mice (Figure 3A and 3B). In the atria, we also found reduced connexin40 in *Hop*^{−/−} compared with *Hop*^{+/−} mice (Figure 3E and 3H). Further, we examined connexin40 protein expression by immunohistochemistry in *Hop*^{+/−} and *Hop*^{−/−} littermates. Areas of intense β-galactosidase activity in adjacent sections were observed in the region of the AVN and proximal CCS, but connexin40 expression was markedly

downregulated in *Hop*$^{-/-}$ as compared with *Hop*$^{+/-}$ mice in all observed sections through the CCS. This difference was most dramatic in the more distal portions of the CCS (Figure 3D and 3G).

Discussion

Disease of the CCS is common and can result from congenital abnormalities or can be acquired later in life. As such, a better understanding of the basic biology and molecular pathways underlying cardiac conduction tissue development, maintenance, and function may have significant impact on the clinical care of patients with conduction disorders.

In this report, we show that *Hop* is highly expressed in the adult CCS of mice and modulates cardiac conduction system function. *Hop* is a transcriptional target of *Nkx2–5*, which is also highly expressed in the CCS[12] and is required for normal development and maintenance of adult cardiac conduction tissue.[4,5] Mutations in *Nkx2–5* are associated with proximal conduction system defects in humans and with congenital heart disease.[6] Tissue-specific inactivation of *Nkx2–5* in adult mouse hearts leads to progressive loss of conduction tissue and downregulation of *Hop*.[4] Our data suggest that *Hop* is robustly expressed in the adult CCS. However, unlike *Nkx2–5*, *Hop* does not appear necessary for maintenance or survival of conduction tissue, because the size and integrity of the AVN and His-bundle were normal in *Hop*$^{-/-}$ mice.

Although both *Nkx2–5* and *Hop* mutant mice display conduction system disease, the precise location of conduction delay appears different. Although the AH interval was longer in *Hop*$^{-/-}$ mice compared with *Hop*$^{+/+}$ mice, albeit not significantly, the PR intervals between the two groups were almost identical. This suggests no significant alteration in AVN conduction in the absence of *Hop*. On the other hand, the QRS duration was significantly different between these two groups, consistent with the longer HV intervals we observed in *Hop*$^{-/-}$ mice. Therefore, although it has been shown that *Nkx2–5* mutant mice display predominantly proximal conduction defects,[4,5] *Hop* mutant mice appear to have more distal, infrahisian delay. Our electrophysiological observations are consistent with the fact that connexin40 expression is lower, but still present, in the AVN of *Hop*$^{-/-}$ mice and absent from the infrahisian conduction system. These findings are distinct from those found in the absence of *Nkx2–5*, where there is hypoplasia of the CCS with loss of specific connexin expressing cells, but preservation of overall connexin40 density in the remnant CCS.[5] This may reflect a particular sensitivity of the conduction tissue just below the His-bundle to *Hop* function or to loss of connexin40 expression.[19]

In addition, atrial electrophysiological defects (increased p-wave duration and prolonged AERP) were observed in the absence of *Hop*. Our observed downregulation of connexin40, the major connexin in the atrium, likely contributes to slowed atrial conduction but not to increased refractoriness. Increased refractoriness is predominantly a function of increased action potential duration, which is determined largely by transmembrane ionic fluxes. We are currently investigating the role of *Hop* in regulating transmembrane ionic currents in the heart. The electrophysiological defects reported in this study are not likely to be secondary to structural heart disease because *Hop*$^{-/-}$ mice have normal hemodynamics, as assessed by invasive analysis,[9] and have normal cardiac structure and function as assessed by cardiac-gated MRI.

Taken together, these results support the existence of a molecular hierarchy in which *Nkx2–5* functions upstream of *Hop* with conservation of this molecular program between embryonic myocardium and adult conduction tissue. *Hop* is likely to mediate some, but not all, downstream functions of *Nkx2–5* in cardiac conduction tissues and suggests that individual

segments of the adult CCS are regulated by separate molecular programs. Further characterization of the molecular programs involved with CCS function and maintenance should lead to improved diagnosis and therapy of conduction system disease.

References

1. Cheng G, Litchenberg WH, Cole GJ, Mikawa T, Thompson RP, Gourdie RG. Development of the cardiac conduction system involves recruitment within a multipotent cardiomyogenic lineage. Development 1999;126:5041–5049. [PubMed: 10529421]

2. Gourdie RG, Wei Y, Kim D, Klatt SC, Mikawa T. Endothelin-induced conversion of embryonic heart muscle cells into impulse-conducting Purkinje fibers. Proc Natl Acad Sci U S A 1998;95:6815–6818. [PubMed: 9618495]

3. Rentschler S, Zander J, Meyers K, France D, Levine R, Porter G, Rivkees SA, Morley GE, Fishman GI. Neurogulin-1 promotes formation of the murine cardiac conduction system. Proc Natl Acad Sci U S A 2002;99:10464–10469. [PubMed: 12149465]

4. Pashmforoush M, Lu JT, Chen H, Amand TS, Kondo R, Pradervand S, Evans SM, Clark B, Feramisco JR, Giles WR, Ho SY, Benson DW, Siberbach M, Shou W, Chien KR. Nkx2–5 pathways and congenital heart disease: loss of ventricular myocyte lineage specification leads to progressive cardiomyopathy and complete heart block. Cell 2004;117:378–386.

5. Jay PY, Harris BS, Maguire CT, Buerger A, Wakimoto H, Tanaka M, Kupershmidt S, Roden DM, Schultheiss TM, O'Brien TX, Gourdie RG, Berul CI, Izumo S. Nkx2–5 mutation causes anatomic hypoplasia of the cardiac conduction system. J Clin Invest 2004;113:1130–1137. [PubMed: 15085192]

6. Schott JJ, Benson DW, Basson CT, Pease W, Silberbach GM, Moak JP, Maron BJ, Seidman CE, Seidman JG. Congenital heart disease caused by mutations in the transcription factor NKX2–5. Science 1998;281:108–111. [PubMed: 9651244]

7. Chen F, Kook H, Milewski R, Gitler AD, Lu MM, Li J, Nazarian R, Schnepp R, Jen K, Biben C, Runke G, Mackay JP, Novotny J, Schwartz RJ, Harvey RP, Mullins MC, Epstein JA. Hop is an unusual homeobox gene that modulates cardiac development. Cell 2002;110:713–723. [PubMed: 12297045]

8. Shin CH, Liu ZP, Passier R, Zhang CL, Wang DZ, Harris TM, Yamagishi H, Richardson JA, Childs G, Olson EN. Modulation of cardiac growth and development by HOP, an unusual homeodomain protein. Cell 2002;110:725–735. [PubMed: 12297046]

9. Kook H, Lepore JJ, Gitler AD, Lu MM, Wing-Man Yung W, Mackay J, Zhou R, Ferrari V, Gruber P, Epstein JA. Cardiac hypertrophy and histone deacetylase-dependent transcriptional repression mediated by the atypical homeodomain protein Hop. J Clin Invest 2003;112:863–871. [PubMed: 12975471]

10. Rentschler S, Vaidya DM, Tamaddon H, Degenhardt K, Sassoon D, Morley GE, Jalife J, Fishman GI. Visualization and functional characterization of the developing murine cardiac conduction system. Development 2001;128:1785–1792. [PubMed: 11311159]

11. Kupershmidt S, Yang T, Anderson ME, Wessels A, Niswender KD, Magnuson MA, Roden DM. Replacement by homologous recombination of the minK gene with lacZ reveals restriction of minK expression to the mouse cardiac conduction system. Circ Res 1999;84:146–152. [PubMed: 9933245]

12. Thomas PS, Kasahara H, Edmonson AM, Izumo S, Yacoub MH, Barton PJ, Gourdie RG. Elevated expression of Nkx-2.5 in developing myocardial conduction cells. Anat Rec 2001;263:307–313. [PubMed: 11455540]

13. Brown CB, Feiner L, Lu MM, Li J, Ma X, Webber AL, Jia L, Raper JA, Epstein JA. PlexinA2 and semaphorin signaling during cardiac neural crest development. Development 2001;128:3071–3080. [PubMed: 11688557]

14. El-Badawi A, Schenk EA. Histochemical methods for separate, consecutive and simultaneous demonstration of acetylcholinesterase and nor-epinephrine in cryostat sections. J Histochem Cytochem 1967;15:580–588. [PubMed: 4863647]

15. Berul CI, Aronovitz MJ, Wang PJ, Mendelsohn ME. In vivo cardiac electrophysiology studies in the mouse. Circulation 1996;94:2641–2648. [PubMed: 8921812]

16. Patel VV, Arad M, Moskowitz IPG, Maguire CT, Branco D, Seidman JG, Seidman CE, Berul CI. Electrophysiological characterization and postnatal development of ventricular preexcitation in a mouse familial WPW model. J Am Coll Cardiol 2003;42:942–951. [PubMed: 12957447]

17. Kramer K, van Acker SA, Voss HP, Grimbergen JA, van der Vijgh WJ, Bast A. Use of telemetry to record electrocardiogram and heart rate in freely moving mice. J Pharmacol Toxicol Methods 1993;30:209–215. [PubMed: 8123902]

18. Zhou R, Pickup S, Glickson J, Scott C, Ferarri VA. Assessment of global and regional myocardial function in the mouse using cine and tagged MRI. Magn Reson Med 2003;49:760–764. [PubMed: 12652548]

19. VanderBrink BA, Sellitto C, Saba S, Link MS, Zhu W, Homoud MK, Estes NA 3rd, Paul DL, Wang PJ. Connexin40-deficient mice exhibit atrioventricular nodal and infra-Hisian conduction abnormalities. J Cardiovasc Electrophysiol 2000;11:1270–1276. [PubMed: 11083248]
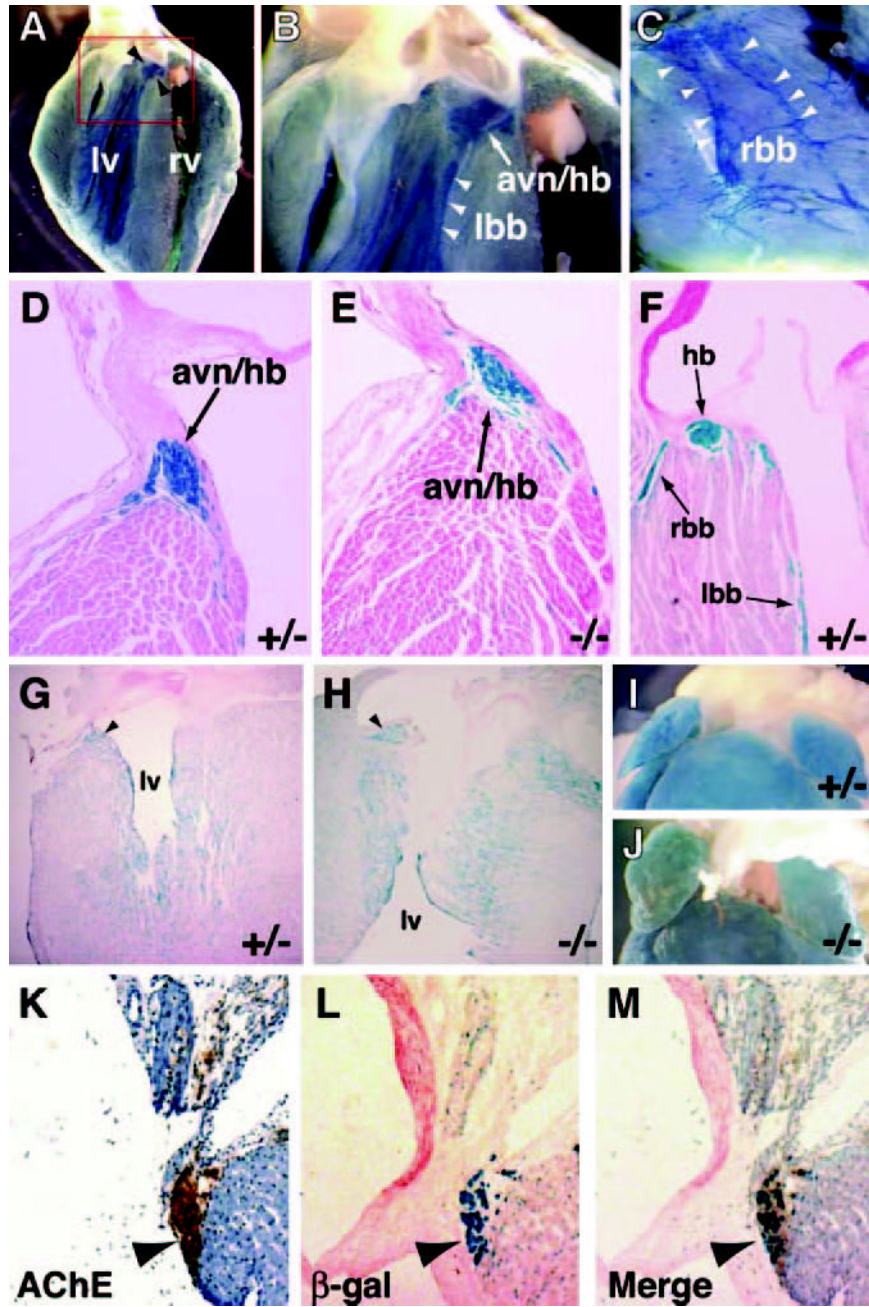
Figure 1.
Hop expression in the murine CCS. A through C, β-Galactosidase staining of *Hop*$^{-/-}$ hearts, demonstrating staining of the ventricular myocardium with strong staining in the CCS (arrowheads). Left and right ventricles (lv, rv) are marked. B, Enlargement of box in A, demonstrating the atrioventricular node and His-bundle (avn/hb) and left bundle branch (lbb, arrowheads). C, Right ventricular septal view of another *Hop*$^{-/-}$ heart, showing strong staining of the right bundle branch (rbb, arrowheads). D through F, Microscopic evaluation of the CCS in *Hop*$^{+/-}$ (D and F) and *Hop*$^{-/-}$ (E) adult mice. F, β-Galactosidase staining of the His-bundle (hb) and right and left bundle branches (rbb, lbb) of a *Hop*$^{+/-}$ mouse heart. Homozygous mice appeared similar (data not shown). G and H, Frozen sections of the hearts of newborn *Hop*$^{+/-}$ (G) and *Hop*$^{-/-}$ (H) littermates, stained for β-galactosidase activity after sectioning.

These sections demonstrate a more restrictive pattern of expression as compared with the global cardiac expression seen at E12.5.[7] There is more prominent staining of the endocardium and proximal CCS (arrowhead) as compared with the rest of the myocardium. This myocardial staining is more pronounced than that seen in adults (A through F). lv indicates left ventricular cavity. I and J, β-Galactosidase activity in *Hop* mutant atria. Grossly stained hearts from adult *Hop*$^{+/-}$ (I) and *Hop*$^{-/-}$ (J) mice, demonstrating strong β-galactosidase activity in the atria. There was no observed area of increased activity within the atria, such as the region of the sinoatrial node. K through M, *Hop* expression compared with AchE activity. K, Proximal His-bundle (arrowhead) of the heart from an adult *Hop*$^{-/-}$ mouse stained for AChE activity (brown). L, β-Galactosidiase expression (blue) in an adjacent section of the heart from (K). There is subtle staining of the muscle and very strong staining of the His-bundle (arrowhead). M, Overlay of images from K and L, demonstrating colocalization of the AChE and β-galactosidase activities in the His bundle (arrowhead).
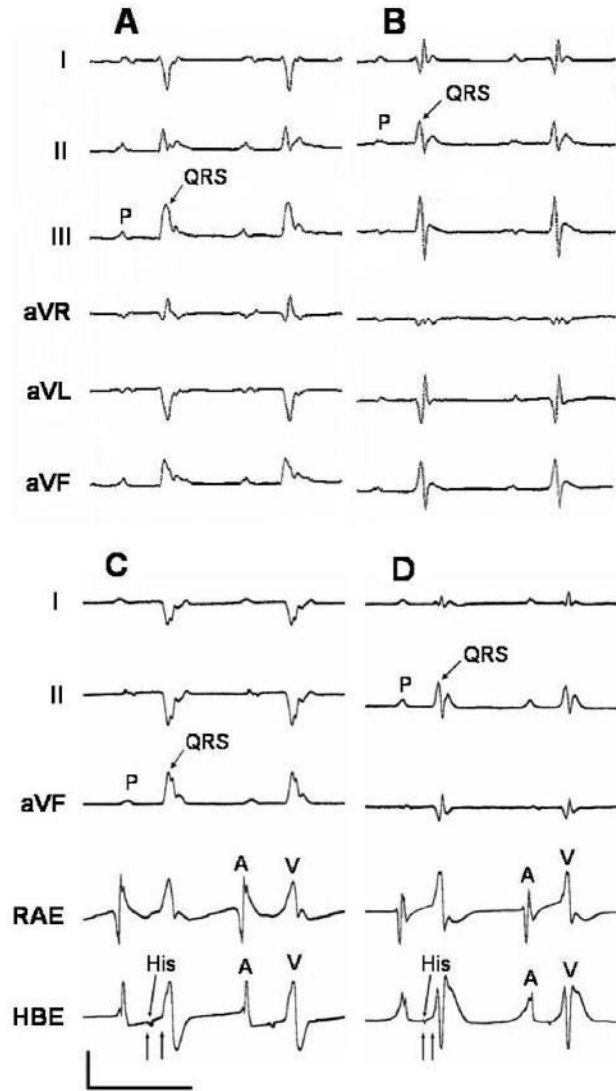
Figure 2.
Conduction defects in adult *Hop*$^{-/-}$ mice. A and B, Surface ECG leads I, II, and III. aVR, aVL, and aVF from a *Hop*$^{-/-}$ (A) and *Hop*$^{+/+}$ (B) mouse show QRS-complex widening, QT-interval prolongation, and p-wave widening in the absence of *Hop*. Right axis deviation is present in the *Hop*$^{-/-}$ mouse vs the Hop$^{+/+}$ mouse. C and D, Intracardiac electrophysiological recording, with surface ECG leads I, II, aVF, the right atrial electrogram (RAE), and His-bundle electrogram (HBE) from a *Hop*$^{-/-}$ (C) and *Hop*$^{+/+}$ mouse (D), demonstrating prolongation of the Hisioventricular (HV) interval in the absence of *Hop. Hop*$^{-/-}$ mouse has a HV-interval of 15 ms vs 10 ms for the *Hop*$^{+/+}$ mouse. Vertical scale bar=1 mV; Horizontal scale bar=100 ms.
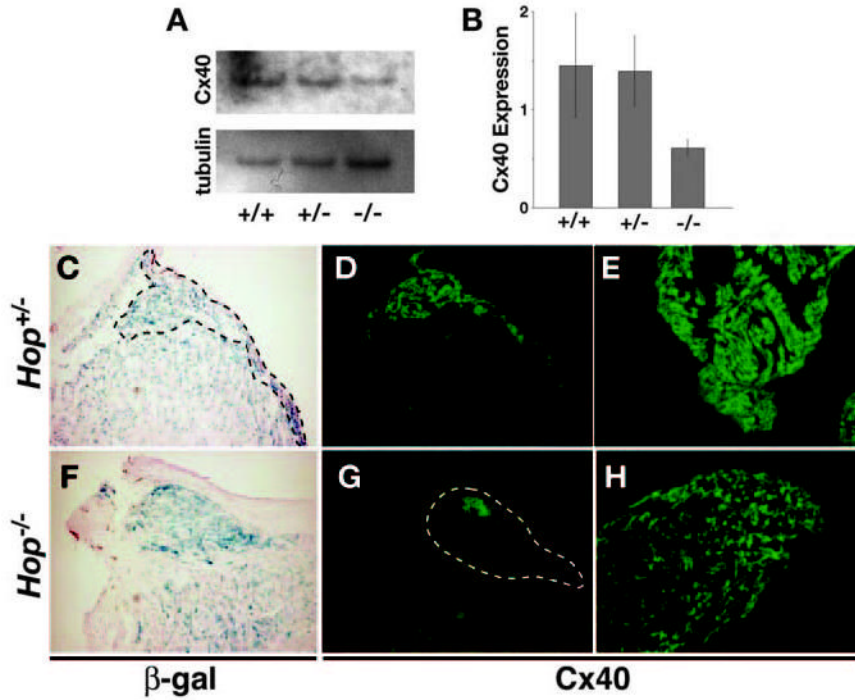
Figure 3.
Connexin40 expression in *Hop* mutant mice. A and B, Western blot analysis of connexin40 expression in the superior septum. A, Sample blot with *Hop* genotypes as indicated. B, Expression of connexin40 in three separate blots normalized to α-tubulin expression, ± SEM. There is a reduction in the relative expression of connexin40 in $Hop^{-/-}$ mice as compared with $Hop^{+/+}$ and $Hop^{+/-}$ littermates. C through H, Immunohistochemistry of the CCS in *Hop* mutant mice. Serial frozen sections of newborn $Hop^{+/-}$ (C through E) and $Hop^{-/-}$ (F through H) hearts were stained for β-galactosidase activity (C and F) and connexin40 (D and E, G and H). Areas of the CCS are outlined. Although there was strong expression of connexin40 seen in the $Hop^{+/-}$ CCS (D), the $Hop^{-/-}$ CCS showed expression of connexin40 in a much smaller area that did not extend beyond the proximal AVN and His-bundle (G). This pattern was noted on several serial sections. E and H, Connexin40 staining in *Hop* mutant atria. Frozen sections of newborn $Hop^{+/-}$ (E) and $Hop^{-/-}$ (H) mice stained together show reduced intensity of staining in the $Hop^{-/-}$ atrium as compared with $Hop^{+/-}$ mice. This finding was observed throughout the atria. All sections were photographed at the same magnification (20× CCS, 10× atria).

TABLE 1

Cardiac-Gated MRI Data

	Hop$^{+/+}$ (n=3)	*Hop*$^{-/-}$ (n=3)
EF, %	65.0±6.2	69.7±10.1
LV mass, mg	107±14.2	112.3±12.7
Wall thickness, mm	0.092±0.008	0.104±0.008

Mean values±SEM.

[*]*P*<0.05 for *Hop*$^{-/-}$ vs *Hop*$^{+/+}$ mice.

TABLE 2

Proximal CCS Volume Measurements

	$Hop^{+/+}$ (n=3)	$Hop^{-/-}$ (n=1)	$Hop^{-/-}$ (n=1)
ECG defect	No	Yes	No
Heart weight, mg	194±30	229	230
CCS vol, ×10^6 μ^3	14.5±0.4	16.9	17.3
CCS vol/heart wt	74.9±14.7	73.8	75.2

Mean values for $Hop^{+/+}$ are ±SEM.

TABLE 3

Surface ECG Data Summary

	Sedated 6-Lead ECG		Conscious Telemetry ECG	
	$Hop^{-/-}$ (n=10)	$Hop^{+/+}$ (n=11)	$Hop^{-/-}$ (n=4)	$Hop^{+/+}$ (n=4)
Age, days	85.4±18.5	82.6±15.5	80.3±6.8	79.0±5.5
Weight, g	26.3±3.1	28.1±2.5	26.7±2.9	25.9±2.1
SCL, ms	155±43.0	147±10.3	103±18.8	101±12.5
HR, bpm	387±102	408±43.2	583±30.1	594±24.5
PR, ms	41.8±6.0*	40.1±4.3	36.7±7.6	37.4±6.3
P-wave, ms	13.7±1.8*	12.4±1.4	12.6±1.2*	11.2±1.0
QRS, ms	13.8±2.3†	10.9±1.1	12.6±1.8†	10.0±0.9
QT, ms	35.3±4.1*	30.5±3.6	33.2±3.4*	29.1±3.1
QTm, ms	29.9±2.2*	26.8±2.0	32.7±2.2*	29.0±1.9
Right Axis Dev	5/10	0/11	2/4	0/4

*
$P<0.05$ for $Hop^{-/-}$ vs $Hop^{+/+}$ mice,

†
$P<0.01$ for $Hop^{-/-}$ vs $Hop^{+/+}$ mice.

SCL indicates sinus cycle length; HR, heart rate; PR, PR-interval duration; QRS, QRS-complex width; QT, QT-interval duration; QTm, corrected QT-interval duration.

TABLE 4

Invasive EP Data Summary

	$Hop^{+/+}$ (n=11)	$Hop^{-/-}$ (n=10)
SCL, ms	153±20.8	182±47.4
HR, bpm	399±57.7	347±80.0
AH, ms	31.0±5.4	36.5±8.3
H_d, ms	4.2±0.8	5.2±1.0
HV, ms	10.5±1.0	13.2±1.5[†]
AVI, ms	39.0±6.6	47.9±8.5*
$SNRT_{120}$, ms	195±36.1	200±43.5
$SNRT_{100}$, ms	186±38.4	215±39.9
$AVERP_{120}$, ms	80.0±10.4	75.0±16.6
AVWBCL, ms	100±14.7	103±14.6
AVN 2:1	80.7±12.1	81.9±12.8
$AERP_{120}$, ms	41.4±7.5	50.0±6.5*
$AERP_{100}$, ms	40.7±6.7	49.8±7.1*
$VERP_{120}$, ms	44.2±7.4	47.5±4.2
$VERP_{100}$, ms	41.4±16.8	43.1±11.0
Duration AT, ms	143±25.9	184±43.8
AT CL, ms	38.1±9.7	32.4±12.2
AT/Mouse	0.5	0.5
Duration VT, ms	270±25.6	297±30.2
VT CL, ms	58.5±6.0	55±8.5
VT/Mouse	0.25	0.25

Symbols are the same as described for Table 1. AH indicates atriohisian interval; Hd, His-duration; HV, hisioventricular interval; AVI, atrioventricular interval; $SNRT_{120}$, sinus node recovery time at drive train of 120 ms; $SNRT_{100}$, sinus node recovery time at drive train of 100 ms; $AERP_{120}$, Atrial ERP at drive train of 120 ms; $AERP_{100}$, atrial ERP at drive train of 100 ms; $AVERP_{120}$, atrioventricular ERP, drive train 120 ms; AVWBCL, AV Wenckebach block cycle length; AV 2:1, AV 2:1 block cycle length; VAWBCL, ventriculoatrial Wenckebach block cycle length; $VERP_{120}$, ventricular ERP at drive train of 120 ms; $VERP_{100}$, ventricular ERP at drive train of 100 ms.